Cell Proliferation

Cell Prolif., 2010, **43**, 445–456 doi: 10.1111/j.1365-2184.2010.00694.x

Cell proliferation of human bone marrow mesenchymal stem cells on biodegradable microcarriers enhances *in vitro* differentiation potential

L.-Y. Sun*, D.-K. Hsieh†, W.-S. Syu‡, Y.-S. Li‡, H.-T. Chiu* and T.-W. Chiou‡

**Department of Biological Science and Technology, National Chiao Tung University, Hsinchu, Taiwan, †Department of Applied Chemistry, Chaoyang University of Technology, Taichung, Taiwan, and ‡Department of Life Science and Graduate Institute of Biotechnology, National Dong Hwa University, Hualien, Taiwan*

Received 17 *October* 2009; *revision accepted* 12 *January* 2010

Abstract

Objectives: For reasons of provision of highly-specific surface area and three-dimensional culture, microcarrier culture (MC) has garnered great interest for its potential to expand anchorage-dependent stem cells. This study utilizes MC for *in vitro* expansion of human bone marrow mesenchymal stem cells (BMMSCs) and analyses its effects on BMMSC proliferation and differentiation.

Materials and methods: Effects of semi-continuous MC compared to control plate culture (PC) and serial bead-to-bead transfer MC (MC bead-T) on human BMMSCs were investigated. Cell population growth kinetics, cell phenotypes and differentiation potential of cells were assayed.

Results: Maximum cell density and overall fold increase in cell population growth were similar between PCs and MCs with similar starting conditions, but lag period of BMMSC growth differed substantially between the two; moreover, MC cells exhibited reduced granularity and higher CXCR4 expression. Differentiation of BMMSCs into osteogenic and adipogenic lineages was enhanced after 3 days in MC. However, MC bead-T resulted in changes in cell granularity and lower osteogenic and adipogenic differentiation potential.

Conclusions: In comparison to PC, MC supported expansion of BMMSCs in an up-scalable three-dimensional culture system using a semi-continuous process, increasing potential for stem cell homing ability and osteogenic and adipogenic differentiation.

Correspondence: T.-W. Chiou, PhD, Department of Life Science and Graduate Institute of Biotechnology, National Dong Hwa University, No. 1, Sec. 2, Da Hsueh Rd., Shou-Feng, Hualien, Taiwan. Tel.: 886-3-8633638; Fax: 886-3-8630398; E-mail: twchiou@mail.ndhu.edu.tw

H.-T. Chiu, PhD, Department of Biological Science and Technology, National Chiao Tung University, No. 75, Po-Ai St., Hsinchu, Taiwan. Tel.: 886-3-5131595; Fax: 886-3-5719605; E-mail: chiu@mail.nctu.edu.tw

Introduction

Bone marrow mesenchymal stem cells (BMMSCs) have been recognized to constitute a powerful tool in regenerative medicine due to their multi-lineage differentiation ability (1,2) and their capacity for tissue repair (3–5). However, as a successful cell treatment requires at least 10^9 functional cells per human adult patient (6,7), human BMMSC therapies would not be a viable option without a practical and up-scalable bioprocess that allows expansion and recovery of high-quality cells.

Extended expansion of mesenchymal stem cells (MSCs) in two-dimensional plate culture (PC) does not produce sufficient numbers of cells for therapeutic applications and leads to their senescence and loss of multipotency (8–10). Recently, microcarriers in a suspension culture system have been shown to facilitate expansion of MSCs, that require attachment, and to provide an environment that can be easily controlled and monitored (11–13).

MSCs can attach and proliferate on Cytodex 1, a general-purpose non-biodegradable microcarrier for anchorage-dependent cell lines (11). However, highly efficient separation of the cells from Cytodex 1 after enzyme treatment is difficult to achieve and Cytodex 1 cannot be degraded by the human body (14). Thus, biodegradable substances such as gelatin-based CultiSpher microcarriers have elicited more interest and have been extensively studied for MSC culture (13,15).

Recently, multipotency of rat MSCs has been shown to be preserved in cultures with Cultispher-S (8×10^5 beads/g) microcarriers using semi-continuous (13) or bead-to-bead transfer (15) process. In comparison with Cultispher-S, CultiSpher-G (1×10^6 beads/g) provides a higher specific surface area (surface area per

gram) and it is composed of cross-linked porcine gelatin. These microcarriers can be dissolved with trypsin-EDTA or collagenase and almost all cells grown on them can be recovered for cell transplantation or tissue engineering (14).

The aim of this study was to analyse different characteristics of human BMMSCs after CultiSpher-G microcarrier culture (MC) and enzyme treatment compared to human BMMSCs maintained in PC. We investigated influence of MC on cell proliferation, morphology, population size, surface marker expression and differentiation potential of human BMMSCs.

Materials and methods

Control plate culture

Phenotypic characteristics of human BMMSCs maintained in PC have been described previously (4,16). Here, cells between passages 10 and 12 were used for all experiments. For control PCs, BMMSCs were seeded at three initial cell densities (6.7×10^3, 1.1×10^4 and 2.2×10^4 cells/cm^2) in six-well plates (BD Falcon™; BD Biosciences, Mississauga, ON, Canada) with BMMSC expansion medium (16) for 7 days (Table 1). Beginning on day 3, medium would be completely changed every 3 days. All cultures were maintained at 37 °C in a humidified 5% CO_2 incubator.

Microcarrier culture

For MCs, 100- and 500-ml spinner flasks (Bellco Glass Inc., Vineland, NJ, USA) were siliconized with Sigmacote (Sigma, St Louis, MO, USA). CultiSpher-G (130–380 μm in diameter; HyClone, Logan, UT, USA) was weighed, hydrated and sterilized by autoclaving as recommended by the manufacturer (15 min, 121 °C), to obtain final concentrations designated for each culture condition. Microcarriers were equilibrated in culture medium overnight prior to cell addition to maximize cell attachment (data not shown).

BMMSCs were added to 50 ml expansion medium in 100-ml spinner flasks at the two seeding densities and microcarrier densities, as indicated in Table 1, for 7 days. Cultures were stirred intermittently (25 rpm for 30 min, followed by a 10-min rest) using an external magnetic stirring system (Bell-ennium™ 5-Position Digital Display Magnetic Stirrer, Bellco Glass) for 2 h to improve cell attachment (data not shown). After this period, cultures were stirred constantly at 25 rpm. Starting on day 3, medium changes were performed every 3 days. Before changing the medium, microcarriers were allowed to settle for 5 min; 50% supernatant was then discarded and new medium was added. All cultures were maintained at 37 °C in a humidified, 5% CO_2 incubator.

The semi-continuous MC method was compared to a serial bead-to-bead transfer method (MC bead-T) to examine cellular characteristics of BMMSCs maintained by a feeding regime for a total of nine days. BMMSCs were added to 50 ml of expansion medium in 100-ml spinner flasks at initial cell density of 5.0×10^4 cells/ml and microcarrier concentration of 3.0 mg/ml (final initial cell density around 1.1×10^4 cells/cm^2), see Table 1. Starting on day 3, equal amounts of expansion medium with 3.0 mg/ml microcarrier were added every 3 days. When volume of medium was larger than 100 ml, MC of BMMSCs was transferred to a 500-ml spinner flask. Schematic diagram of the three culture processes is shown in Fig. 1.

To monitor location and proliferation of cells on microcarriers, 0.5-ml samples were removed from MCs, rinsed in PBS, fixed for 10 min in 10% formalin at 25 °C and stained by using Hoechst 33342 dye (Invitrogen-Molecular Probes, Carlsbad, CA, USA) in the dark for 2 min to detect nuclei. Samples were then rinsed three times in PBS to eliminate background fluorescence, trans-

Table 1. Initial cell density and available surface area for the control plate and microcarrier culture conditions

Culture type	Fed	CG/ml	Initial cell density		Medium volume (ml)	Available area (cm^2)
			10^4 cells/ml	10^4 cells/cm^2		
PC	–	–	10.66	2.22	2	9.6
			5.33	1.11		
			3.22	0.67		
MC	–	3.0	10.00	2.22	50	∼225
			5.00	1.11		
		5.0	5.00	0.67	50	∼375
MC Bead-T	0	3.0	5.00	1.11	50	∼225
	1		7.35 ± 1.89	1.63 ± 0.42	100	∼450
	2		7.20 ± 0.82	1.60 ± 0.18	200	∼900

CG, CultiSpher-G; MC, microcarrier culture; PC, plate culture.

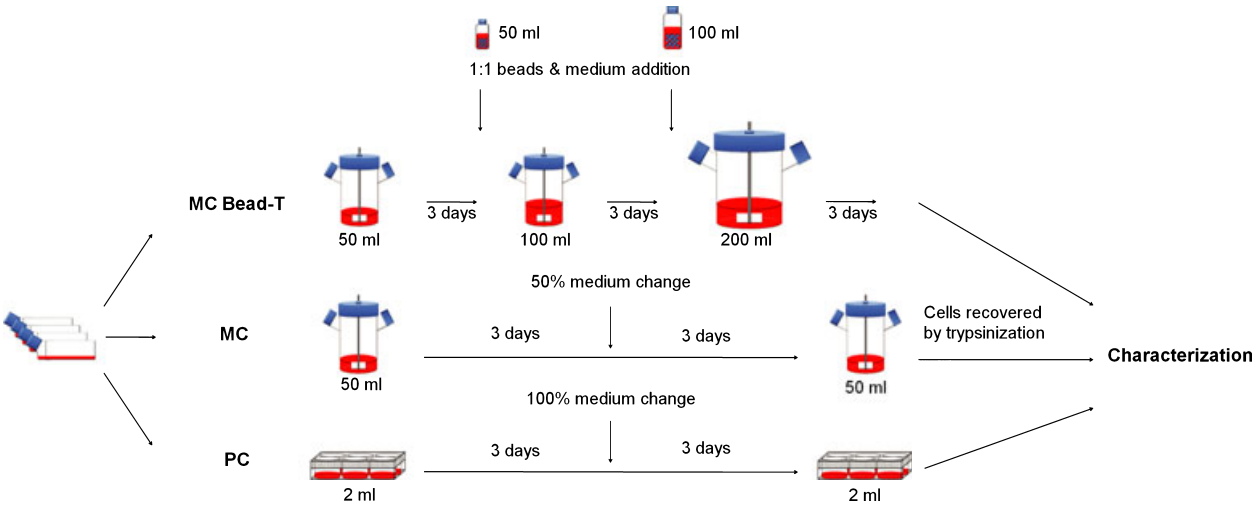

Figure 1. Three culturing conditions used to grow bone marrow mesenchymal stem cells (BMMSCs). Culture protocols are shown for control plate culture (PC), microcarrier culture (MC) and MC with serial bead-to-bead transfer (MC bead-T). Characterization of BMMSCs recovered from PC, MC and MC bead-T was performed before cell death phase of the cultures.

ferred to slides and visualized immediately by a fluorescence microscope (IX70; Olympus, Tokyo, Japan).

Analysis of cell population growth kinetics

For daily cell count of PCs, cells were detached with trypsin-EDTA (Invitrogen-Gibco, Carlsbad, CA, USA) using a cell scraper (BD Biosciences). For daily cell count of MCs, 1.0-ml samples were removed from the spinner flask and allowed to settle for 5 min. Supernatant was removed and the culture was rinsed twice in PBS; cells were incubated in trypsin-EDTA (1 ml) for 10–15 min at 37 °C to dissolve the microcarriers. They were then counted in triplicate using a haemocytometer. Cell viability was measured by trypan blue (Sigma) exclusion.

Cell population growth rate, which is the reciprocal of generation time, was calculated by number of cell doublings per unit time during the specified time interval (16). In this study, calculated maximal cell population growth rate (μ_{max}) represents growth rate of the exponential phase during the culture process and average growth rate (μ_{avg}) represents number of doublings per unit time before death phase.

Supernatant samples were collected throughout cell growth kinetics experiments. After centrifugation, glucose and lactate concentrations in supernatant were measured directly using a glucose/lactate analyser (Model YSI 2700; Yellow. Springs Instrument Co., Yellow Springs, OH, USA). Glucose and lactate concentrations were used for calculation of yield of lactate from glucose ($Y_{Lac/Glc}$) by the following equation: $Y_{Lac/Glc} = \Delta Lactate/\Delta Glucose$, where ΔGlucose is change in glucose over the time period, and ΔLactate is the change in lactate over the time period.

Cell size, granularity and surface markers

To study their morphology and cell population (including cell size, granularity, and surface antigen phenotype), BMMSCs were detached by trypsinization for 10 min, stained with anti-human CXC chemokine receptor 4 fluorescein isothiocyanate (FITC)-conjugated antibodies (CXCR4; R&D Systems, Minneapolis, MN, USA) and analysed using flow cytometry (Cytomics FC500; Beckman Coulter, Fullerton, CA, USA). BMMSCs stained with anti-mouse IgG antibodies FITC-conjugated (Dako, Carpinteria, CA, USA) were used as negative control. Cell size and granularity of BMMSCs from the different culture types were analysed using CytomicsCXP software (Beckman Coulter) at days 0, 3 and 6. Variations in surface marker density (CXCR4) of PC, MC and MC bead-T were analysed using CytomicsCXP software on days 0, 6 and 9.

Osteogenic and adipogenic differentiation

Osteogenesis and adipogenesis were induced by established protocols previously described (16). Cells recovered from PCs and MCs on day 3 and from MCs bead-T on day 6 were replated on to 35-mm dishes (BD Biosciences) at initial cell density of 10^4 cells/cm^2. Osteogenic differentiation potential of BMMSCs was evaluated by measuring alkaline phosphatase (ALP) activity on days 3, 7 and 14. Adipogenic differentiation potential of BMMSCs was evaluated by Oil red O staining and Nile Red flow cytometry, measuring accumulation of lipid vesicles on days 3 and 7. ALP staining and Oil red O staining were carried out as described previously (16).

Quantification of ALP activity

Cells were detached by trypsinization for 10 min, resuspended in deionized water and vortexed for 10 min to disrupt cell membranes. ALP activity was then assayed using an ALP liquicolor kit (HUMAN GmbH, Wiesbaden, Germany) in a 37 °C water bath. Absorbance of *p*-nitrophenol product was measured at 405 nm using a spectrophotometer (GE Healthcare Bio-Sciences Corp., Piscataway, NJ, USA). Specific ALP activity was expressed in U/l/cell.

Nile Red flow cytometry

To determine percentage of BMMSCs in each sample that had undergone adipogenic differentiation, 10^5 cells were detached by trypsinization for 10 min and stained using Nile Red fluorescent dye (Sigma, 0.5 μg Nile Red in 1 ml of 3:1 glycerol/water mixture) for 5 min. Undifferentiated BMMSCs from PCs were also stained with Nile Red fluorescent dye to serve as negative control. Percentage of BMMSCs that had undergone adipogenic differentiation was analysed using CytomicsCXP software.

Total RNA isolation and semi-quantitative reverse transcriptase-polymerase chain reaction

Isolation of total RNA, cDNA synthesis and amplification reactions were carried out as described previously (17,18). To analyse differences in expression levels of osteogenesis-related and adipogenesis-related genes in differentiated BMMSCs, cells from PCs and MCs were replated on to 35-mm dishes at initial density of 10^4 cells/cm^2 and were treated with osteogenic medium for 7 or 14 days, or with adipogenic medium for 3 or 7 days. The cDNA was amplified by PCR with gene-specific primers, as listed in Table 2. Genes amplified included osteopontin (OPN), parathyroid hormone receptor type 1 (PTH-R1), ALP, core binding factor α1 (cbfa1), CCAAT/enhancer-binding protein α (C/EBPα), proliferator-activated receptor γ2 (PPARγ2) and β-actin. To determine levels of mRNA expression, band intensities were analysed using ImageJ software (ImageJ 1.40g, National Institutes of Health, Bethesda, MD, USA). Gene expression levels were normalized to β-actin, which was amplified as internal control.

Statistical analyses

Statistical analyses of cell proliferation, cell population, surface marker density, ALP activity and gene expression level for each group were carried out using Microsoft Excel data analysis program for *t*-test analysis; *P*-value <0.05 was considered statistically significant. Experiments were performed at least twice. Results are expressed as the mean ± SD (n = 3).

Results

Comparison of cell population growth kinetics and metabolic parameters from different human BMMSC culturing conditions

To study cell populations of BMMSCs and their growth in MC, cells were seeded at three different culture conditions

Table 2. Primers used for RT-PCR

Gene name	Primer sequence	Product (bp)
β-actin	F: 5′-CGCCAACCGCGAGAAGAT-3′ R: 5′-CGTCACCGGAGTCCATCA-3′	168
ALP	F: 5′-TGGAGCTTCAGAAGCTCAACACCA-3′ R: 5′-ATCTCGTTGTCTGAGTACCAGTCC-3′	454
cbfa1	F: 5′-CTCACTACCACACCTACCTG-3′ R: 5′-TCAATATGGTCGCCAAACAGATTC-3′	320
OPN	F: 5′-CATCTCAGAAGCAGAATCTCC-3′ R: 5′-CCATAAACCACACTATCACCTC-3′	313
PTH-R1	F: 5′-CACAGCCTCATCTTCATGG-3′ R: 5′-GCATCTCATAGTGCATCTGG-3′	357
C/EBPα	F: 5′-GTCGGTGGACAAGAACAGC-3′ R: 5′-ATGGCCTTGACCAAGGAGC-3′	234
PPARγ2	F: 5′-GCTGTTATGGGTGAAACTCTG-3′ R: 5′-ATAAGGTGGAGATGCAGGCTC-3′	351

ALP, alkaline phosphatase; C/EBPα, CAAT/enhancer-binding protein α; cbfa1, core binding factor alpha 1; F, forward; OPN, osteopontin; PPARγ2, proliferator-activated receptor γ2; PTH-R1, parathyroid hormone receptor type 1; R, reverse.

(Table 1). Optically sectioned gelatin beads from cultures on days 1, 3 and 6 were visualized using Hoechst staining. Surface-adherent cells were present on day 1 and their numbers increased by day 6, based on the macroporous structures (Fig. 2a).

Initially, proliferation of BMMSCs appeared to be affected by stirring and the three-dimensional environment from MC, but there were no significant differences in cell densities observed on day 6 (Table 3). Lag phase of BMMSC population growth was substantially different between PC and MC growth conditions (Fig. 2b). When cells were plated at initial density of 2.2×10^4 cells/cm^2, cell density of MCs did not increase by day 2; however, density of PCs increased to 4×10^5 cells/cm^2 over the same time (Fig. 2b). The longer lag period of BMMSCs in MC resulted in lower average growth rates as compared to PCs, but maximal population growth rate in MCs was higher than that in PCs with the same initial cell density during log phase (Table 3). Three different initial cell densities of 2.2×10^4, 1.1×10^4 and 6.6×10^3 cells/cm^2 resulted in fold increases in MCs of 2.84, 4.85 and 6.94 respectively, and similar fold increases in PCs of 2.42, 4.77 and 7.99 respectively (Table 3).

As surface area of microcarriers limits cell expansion, we tested serial bead-to-bead transfer in which fresh beads were added when cells become ~60% confluent during the log phase. Viable cell density of MC bead-T derived BMMSCs did not differ much before day 3 (Fig. 2c) as compared to cells grown in PC or MC. Cell density decreased from $3.2–3.0 \times 10^4$ to $1.6–1.5 \times 10^4$ cells/cm^2 upon addition of fresh medium and microcarriers on day 3. An additional lag period of about 1 day was observed after each feeding. After isolating cells from PCs, MCs or MC bead-T by trypsin-EDTA, greater than 92% of cells remained viable as assessed by trypan blue staining, at most time points (Fig. 2b,c). This is in agreement with low frequency of cell death observed after cell retrieval by trypsin-EDTA.

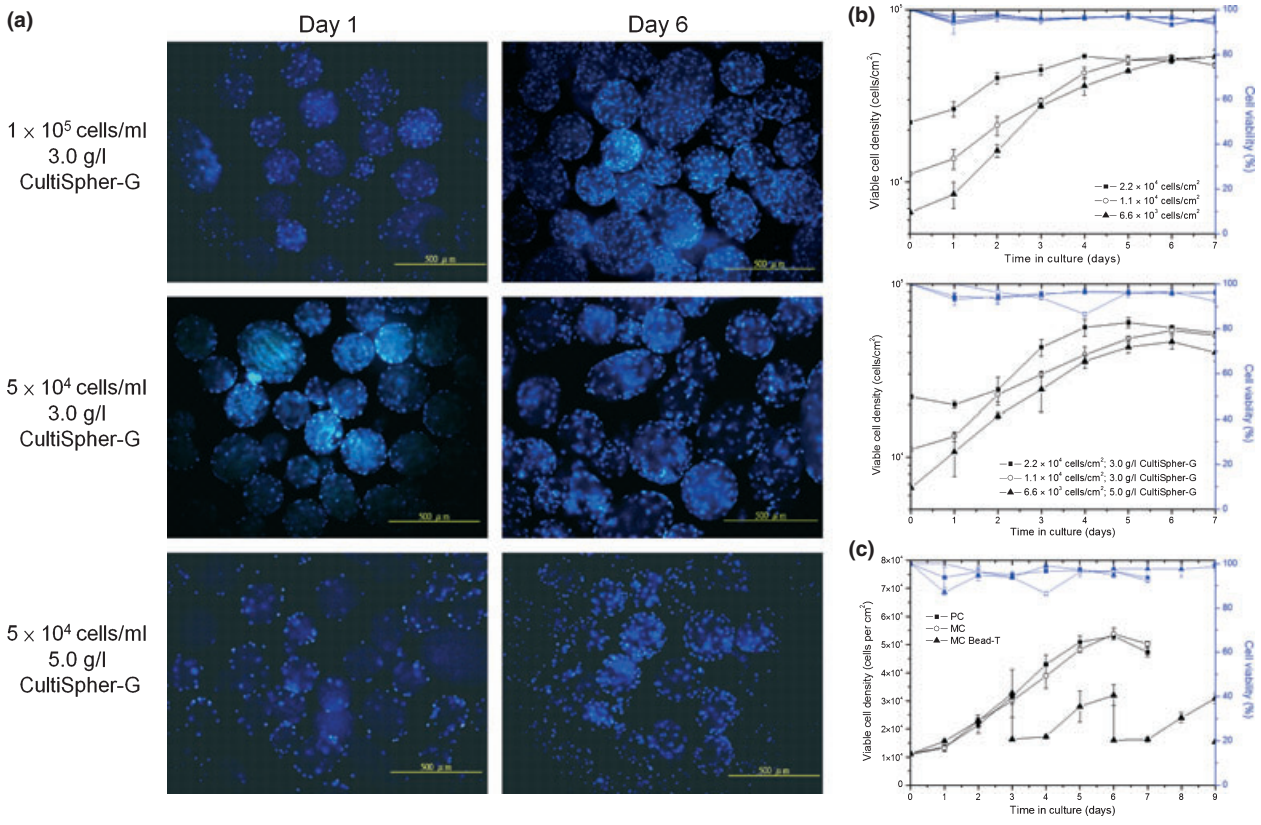

Figure 2. Cell proliferation of BMMSCs grown in MC as compared to cells grown in PC by semi-continuous method. (a) Proliferation of BMMSCs from MCs grown in semi-continuous culture for 7 days at different initial cell densities (top, in cells/ml) and CultiSpher-G concentrations (bottom, in g/l), then stained using Hoechst 33342 dye. Scale bar = 500 μm. (b) Growth kinetics of BMMSCs comparing PCs and MCs with different initial cell densities of 2.22×10^4, 1.11×10^4 and 6.7×10^3 cells/cm^2 ($n = 3$). Data presented in semi-log linear charts by Double-Y plot that includes viable cell density (block lines) and cell viability (blue lines). (c) Viable cell density of BMMSCs in MC bead-T as compared to cells grown in PC and MC at initial cell density of 1.11×10^4 cells/cm^2. Data displayed in linear chart by Double-Y plot that includes viable cell density (block lines) and cell viability (blue lines).

Table 3. Growth kinetics and metabolic parameters obtained from PCs and MCs at day 6 and MC Bead-T at day 9

Culture type	Fed	Initial cell density		Maximal cell density		μ_{avg}[a] (h^{-1})	μ_{max}[b] (h^{-1})	$Y_{Lac/Glc}$[c]	Fold increase
		10^4 cells/ml	10^4 cells/cm^2	10^4 cells/ml	10^4 cells/cm^2				
PC	–	10.66	2.22	25.77 ± 0.29	5.16 ± 0.59	0.047 ± 0.001	0.025 ± 0.009	1.04 ± 0.03	2.42
		5.33	1.11	25.44 ± 0.29	5.09 ± 0.59	0.038 ± 0.001	0.027 ± 0.002	1.18 ± 0.04	4.77
		3.22	0.67	25.59 ± 2.23	5.33 ± 0.47	0.020 ± 0.001	0.036 ± 0.003	1.32 ± 0.05	7.99
MC	–	10.00	2.22	26.90 ± 3.61	5.98 ± 0.80	0.012 ± 0.002	0.034 ± 0.001	0.97 ± 0.06	2.84
		5.00	1.11	24.20 ± 0.94	5.38 ± 0.21	0.016 ± 0.001	0.033 ± 0.009	1.02 ± 0.05	4.85
		5.00	0.67	34.70 ± 3.16	4.63 ± 0.42	0.019 ± 0.004	0.041 ± 0.001	1.14 ± 0.16	6.94
MC Bead-T	0	5.00	1.11	14.70 ± 3.78	3.27 ± 0.84	0.022 ± 0.004	0.043 ± 0.014	0.68 ± 0.02	2.95
	1	7.35 ± 1.89	1.63 ± 0.42	14.40 ± 1.65	3.20 ± 0.37	0.013 ± 0.005	0.028 ± 0.013	0.80 ± 0.03	5.79
	2	7.20 ± 0.82	1.60 ± 0.18	13.90 ± 0.79	3.09 ± 0.17	0.015 ± 0.003	0.023 ± 0.002	1.49 ± 0.12	11.18

CG, CultiSpher-G; MC, microcarrier culture; PC, plate culture.
[a]Average growth rate (μ_{avg}) represents the number of doublings per unit time before the death phase.
[b]Maximal growth rate (μ_{max}) represents the growth rate during the log phase.
[c]$Y_{Lac/Glc}$ indicates the yield of lactate from glucose using the following equation: $Y_{Lac/Glc} = \Delta Lactate/\Delta Glucose$.

To monitor cell metabolism, glucose and lactate consumption were measured. Yield of lactate from glucose ($Y_{Lac/Glc}$) is associated with inefficient metabolism of glucose (Table 3). During the semi-continuous method of culture, yield of lactate from glucose was in the order of 1.04–1.32 g/g for PC and 0.97–1.14 g/g for MC categories. These differences were not statistically significant except for the group with initial cell density of 1.1×10^4 cells/cm^2 ($P < 0.05$). Yield of lactate from glucose increased with initial cell density. Slightly higher $Y_{Lac/Glc}$ yields were obtained from PC as compared to MC when cells were plated at the same initial cell density. For initial cell density of 1.1×10^4 cells/cm^2 and with bead-to-bead transfer, $Y_{Lac/Glc}$ yields of 0.68–1.49 were obtained at each feeding. Although higher $Y_{Lac/Glc}$ was obtained after the second feeding, total $Y_{Lac/Glc}$ for this method (0.96 ± 0.02) was still lower than that of the other groups.

Effects of MC on cell morphology, cell population and immunophenotype

BMMSCs are mostly spindle-shaped while grown at a low density (19). Their morphology after 3 days of PC or MC, or after 6 days of MC bead-T was similar (Fig. 3a). On day 3, there were no significant changes in morphology of BMMSCs from MCs as compared to those from PCs, but some non-spindle-shaped cells (red arrows, Fig. 3a) were observed in PC; these were rarely observed after 3 days in stirred MC with semi-continuous method. However, non-spindle-shaped cells were observed after day 6 in MC bead-T (red arrows, Fig. 3a). We hypothesize that some BMMSCs reached confluency on old beads, resulting in these non-spindle-shaped cells.

BMMSCs grown under different culture conditions were assayed for size and granularity by their forward and side scatter properties on flow cytometry. In PCs at day 3, there were two populations of BMMSCs: A division and B division (Fig. 3b). Percentage of A division was increased and percentage of B division was reduced after 3 days in MC (Table 4). Although the percentage of A division in PCs and MCs both increased after 6 days in culture (when cells reached confluence), differences in the percentage of A division and B division in PCs and MCs were still significant (P-value < 0.05). In addition, there was a concomitant decrease in percentage of granular cells (C2 plus C4 division) over time (Table 4). However, after 3 days in MC, percentage of small and agranular cells (C3 division) was significantly higher than that of cells in PC (P-value <0.005). After 6 days in MC bead-T, percentage of granular cells (C2 plus C4 division) was higher than that in PC (day 3) and MC (day 6), but percentage of A division in MC bead-T was significantly lower than that in PC or MC at day 6 (Table 4). Our data suggest that cell size and cell population of BMMSCs varied depending on the different culture conditions.

BMMSCs were allowed to recover at different intervals after PC and MC, and they were then assayed for surface markers using FITC-coupled antibodies against human CXCR4, by flow cytometry (Fig. 3c). Expression levels of CXCR4 on BMMSCs from PCs and MCs steadily decreased over the course of the 6-day culture period, but BMMSCs from MCs maintained significantly higher CXCR4 density levels and higher ratios of CXCR4-positive cells (CXCR4+: 95.4 ± 6.4%; X-Mean: 44.5 ± 3.7) than did those from PCs (CXCR4+: 86.9 ± 0.5%; X-Mean: 12.9 ± 1.9) at day 3 (log phase; Fig. 3c,

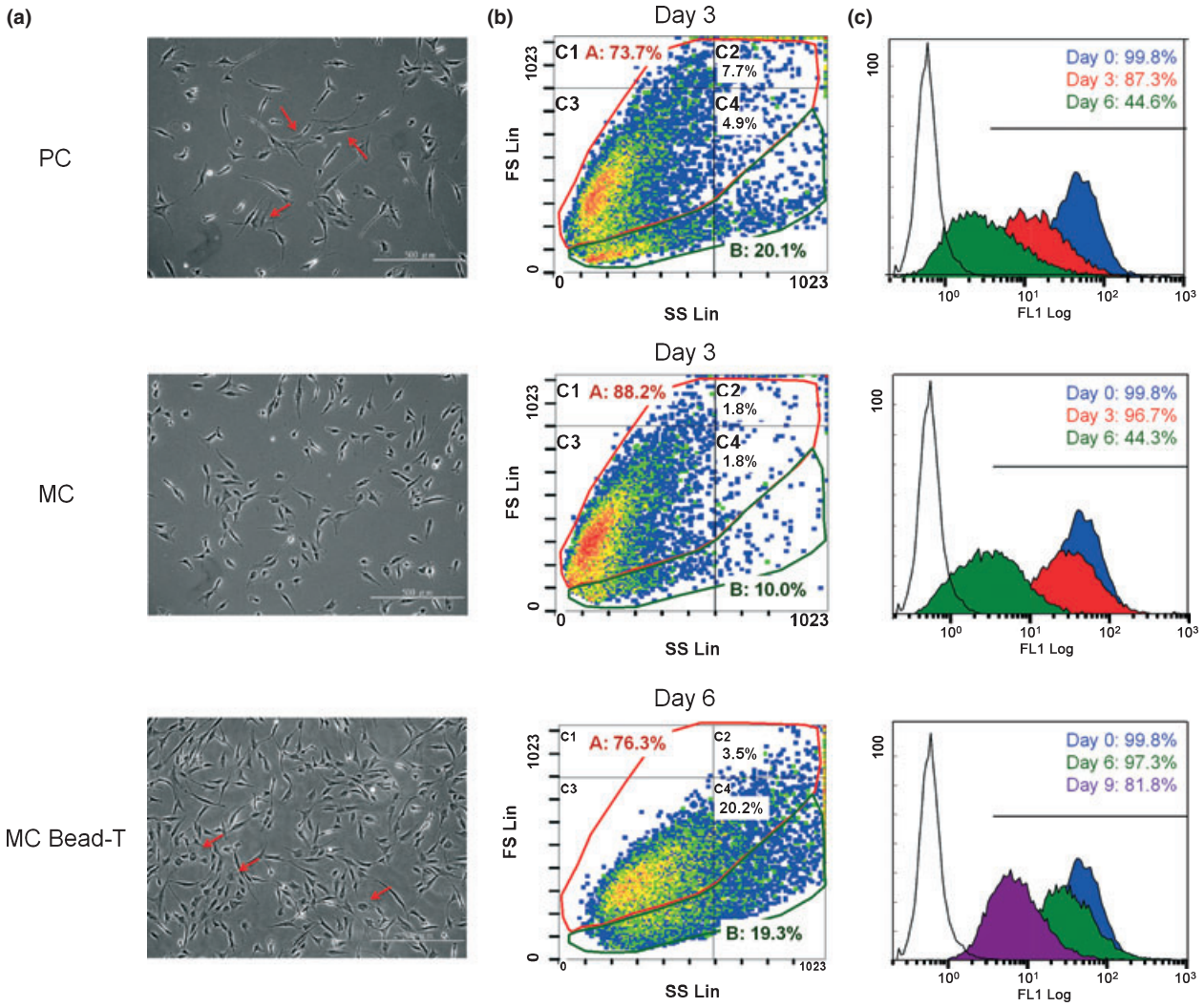

Figure 3. Effects of different cell culture methods on morphology and surface marker density of BMMSCs. (a) Photomicrographs of BMMSCs recovered from PCs and MCs at day 3 and from MCs bead-T at day 6 and replated on to 35-mm dishes for one day (red arrows, non-spindle-shaped cells). (b) Change in cell size and cell population of BMMSCs grown under the different culture conditions analysed by flow cytometry using forward scatter (FS) versus side scatter (SS) density plots. The density plots were divided into A division (red ring) and B division (green ring) based on two populations of BMMSCs present in PCs at day 3 or into C1–C4 divisions based on major populations of BMMSCs in MCs at day 3. Density level threshold, 50 cells, and density levels of 1–5 indicated by colour (blue to red). (c) Variation of surface marker density (CXCR4) of BMMSCs from different culture protocols shown in histogram plots derived from flow cytometry at days 0 (blue), 3 (red), 6 (green) and 9 (purple). Black-line histogram indicates background signal; coloured histograms represent positive reactivity with the CXCR4 antibody.

Table 4). BMMSCs in MC for 3 days did not, however, show significant changes in other surface markers including CD13, CD14, CD29, CD34, CD44, CD45, CD49b, CD49d, CD73, CD90, CD105, HLA-ABC and HLA-DR (data not shown). At day 6, BMMSCs from MCs bead-T maintained significantly higher levels of CXCR4 expression as compared to BMMSCs from PCs or MCs, but intensity of CXCR4 expression density and ratio of CXCR4-positive cells in MCs bead-T were lower than those found at day 0 (Table 4).

Comparison of osteogenic differentiation potential of BMMSCs derived by different culturing conditions

Cells of PC (day 3), MC (day 3), and MC bead-T (day 6) were replated on to 35-mm dishes under osteogenic or adipogenic conditions to examine the effect of microcarriers on BMMSC differentiation potential. For osteogenic differentiation, BMMSCs plated at density of 10^4 cells/cm^2 were induced under osteogenic conditions for 14 days. During this period, BMMSCs exhibited dramatic change

Table 4. The effects of different cell culturing methods on BMMSC cell population and CXCR4 expression level

		Day 3		Day 6			Day 9
Characteristic	Day 0	PC	MC	PC	MC	MC Bead-T	MC Bead-T
A division	82.5 ± 1.4%	78.5 ± 7.3%	90.5 ± 2.8%†	64.2 ± 1.0%	78.8 ± 1.2%‡	83.9 ± 0.3%‡	80.0 ± 1.8%
B division	13.3 ± 1.3%	18.4 ± 6.1%	7.7 ± 2.7%*	33.6 ± 1.3%	21.2 ± 0.7%‡	8.5 ± 1.0%‡	14.1 ± 0.6%
C3 division	81.6 ± 1.4%	85.1 ± 1.0%	95.6 ± 0.1%‡	91.6 ± 6.5%	94.1 ± 4.0%	74.0 ± 1.6%*	82.8 ± 3.2%
CXCR4+	99.2 ± 0.2%	86.9 ± 0.5%	95.4 ± 6.4%‡	44.1 ± 3.4%	44.0 ± 3.0%	95.7 ± 1.2%‡	79.4 ± 2.1%
X-Mean	47.4 ± 0.6	12.9 ± 1.9	44.5 ± 3.7*	5.8 ± 0.2	5.81 ± 0.1	41.1 ± 1.0‡	7.4 ± 0.6

Cell population and CXCR4 expression level of BMMSC from MC or MC Bead-T was compared with that from PC for *t*-test analysis.
X-Mean: mean fluorescence (FITC) intensity of CXCR4-positive cells.
*$P < 0.05$, †$P < 0.01$, ‡$P < 0.005$.

in cell morphology and displayed significant increase in ALP activity, which was confirmed by ALP staining (Fig. 4a) and quantified by spectrophotometry (Fig. 4b). ALP is required in the mineralization process and hydrolyses phosphate-containing substrates to increase local phosphate concentration (20). During the osteogenic period, some cells appeared to be ALP positive and activity of ALP-positive cells from MCs was significantly higher than that from PCs at day 14, but activity of ALP-positive cells from MC bead-T was slightly lower than that from PCs and significantly lower than that from MCs (Fig. 4b).

Comparison of adipogenic differentiation potential of BMMSCs derived from different culturing conditions

To evaluate adipogenic potential, we plated BMMSCs at density of 10^4 cells/cm^2 and induced them under adipogenic conditions for 7 days. At days 3 and 7 post induction, cells from PC, MC and MC bead-T exhibited varying degrees of adipogenesis based on changes in visible accumulation of neutral lipid vacuoles observed by Oil red O staining and quantified by Nile Red flow cytometry (Fig. 5). In contrast to cells from PCs (39.2%), BMMSCs from MCs yielded 83.6% adipocytes that contained lipid droplets at day 3, indicating high level of adipogenic potential. BMMSCs recovered from MCs bead-T yielded 32.8% adipocytes (day 3) and 46.5% (day 7), which was lower than the number of adipocytes in BMMSCs recovered from PCs and MCs.

Osteogenic and adipogenic gene expression in BMMSCs from MC and PC

BMMSCs were recovered from PC and MC (day 3) and then cultured in osteogenic medium. At days 7 and l4, total RNA was isolated and then used for semi-quantitative reverse transcriptase-polymerase chain reaction (RT-PCR) analysis of osteogenesis-related genes (Fig. 6a,c). On

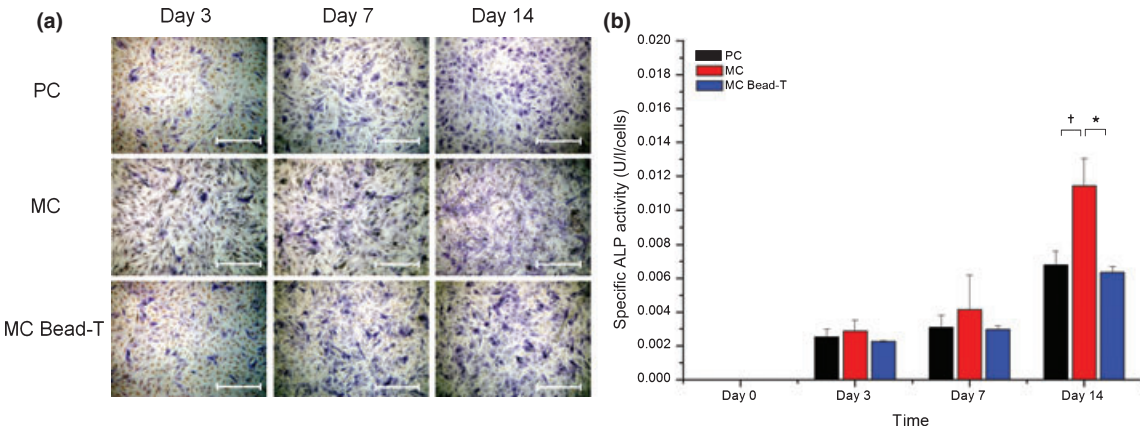

Figure 4. Osteogenic differentiation potential of BMMSCs recovered from PC, MC and MC bead-T. (a) Photomicrographs of ALP activity of BMMSCs grown under different culture conditions as shown by ALP staining. Scale bar = 500 μm. (b) Quantification of specific ALP activity shown by spectrophotometry (O.D. = 405 nm). Results represented as mean ± SD of triplicate cultures from one representative experiment. *$P < 0.05$; †$P < 0.01$.

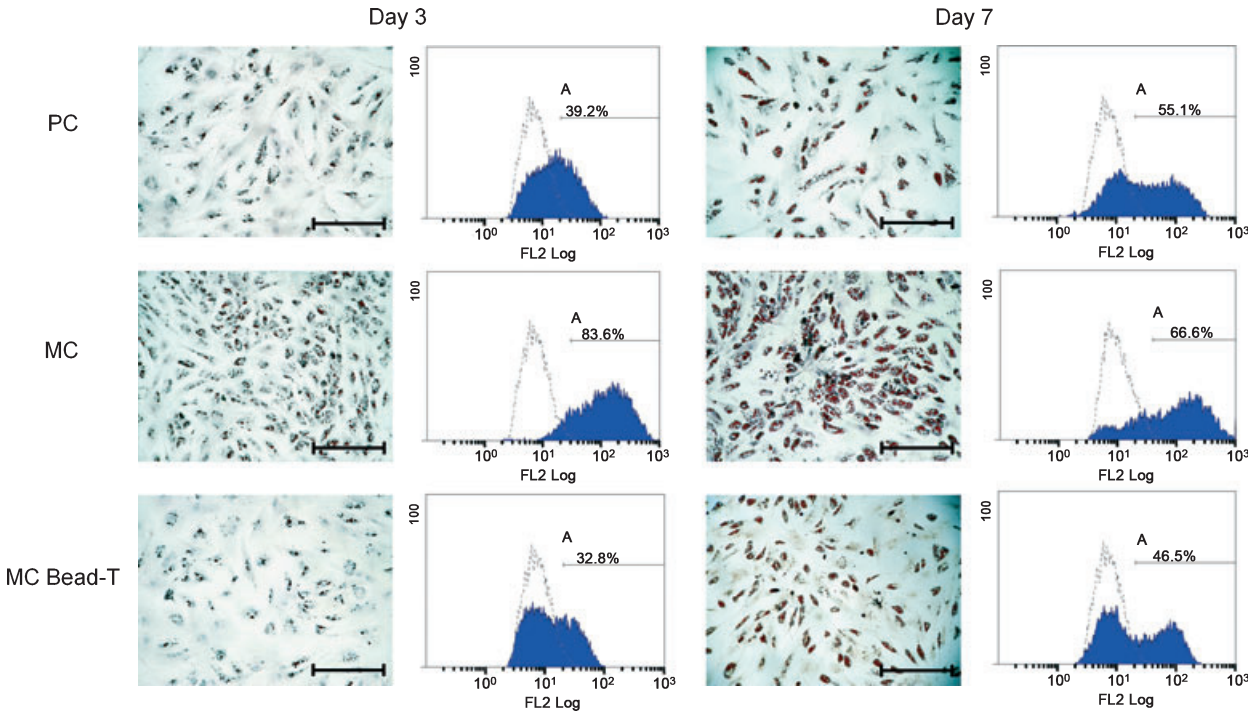

Figure 5. Adipogenic differentiation potential of BMMSCs recovered from PC, MC and MC bead-T. Photomicrographs of lipid spheres in BMMSCs grown in the different culture conditions as shown by Oil red O staining. Scale bar = 500 μm. Quantification of adipo-differentiated BMMSCs (A division) in the different culture types, expressed as percentage of total cells, as derived from Nile Red flow cytometry. Open histogram indicates background signal (undifferentiated BMMSCs stained by Nile Red); blue histogram indicates staining for Nile Red.

day 7, expressions of PTH-R1, ALP, cbfa1, and OPN in BMMSCs from PC were up-regulated. At day 7, BMMSCs from MC showed a similar expression pattern, albeit with a significantly higher level of expression for PTH-R1. On day 14, expressions of PTH-R1, ALP and OPN in cells from PC were further up-regulated and expression of PTH-R1 in cells from MC was still significantly higher than that from PC.

BMMSCs were recovered from PC and MC (day 3) and then cultured in adipogenic medium. At days 3 and 7, total RNA was isolated and then used for semi-quantitative RT-PCR analysis of adipogenesis-related genes (Fig. 6b,d). On day 3, expressions of C/EBPα and PPARγ2 in cells from PC and MC were up-regulated, but expressions of C/EBPα in cells from MC were in the order of 3-fold higher than that in cells from PC. On day 7, expressions of C/EBPα and PPARγ2 in cells from PC and MC were further up-regulated, but expression of PPARγ2 in cells from MC was about 2-fold higher than that in cells from PC.

Discussion

MSCs can retain multipotency and proliferate rapidly at relatively low densities (21–23), but extended expansion of MSCs with low cell densities in two-dimensional PC does not produce sufficient numbers of cells for therapeutic applications. Thus, we used different seeding densities and different CultiSpher-G concentrations to examine culture parameters for optimal expansion of BMMSCs in MC. Cell population kinetics of BMMSC growth in MC differed from their growth kinetics in PC. In PC, BMMSC expansion began with a 1-day lag phase and then entered log phase of exponential growth, although growth rates of cells in the three different seeding densities were almost identical during the lag phase. In contrast, length of lag phase was inversely proportional to initial seeding density for MC. This phenomenon resulted in lower average growth rate for BMMSCs expanded in MCs, as compared to those in PCs. With the same seeding densities, maximum growth rate was higher in MC, although maximum cell density and fold increase at the end of the experiment were similar between the two groups.

Accumulation of lactate is associated with inefficient glucose metabolism (24). To prevent cell growth inhibition by accumulation of metabolites such as lactate and/or deficiency in nutrients such as glucose, feeding regimen should be optimized (25,26). In our study, a slightly higher $Y_{Lac/Glc}$ of 1.04–1.32 g/g was obtained from PC as compared to $Y_{Lac/Glc}$ of 0.97–1.14 g/g from MC,

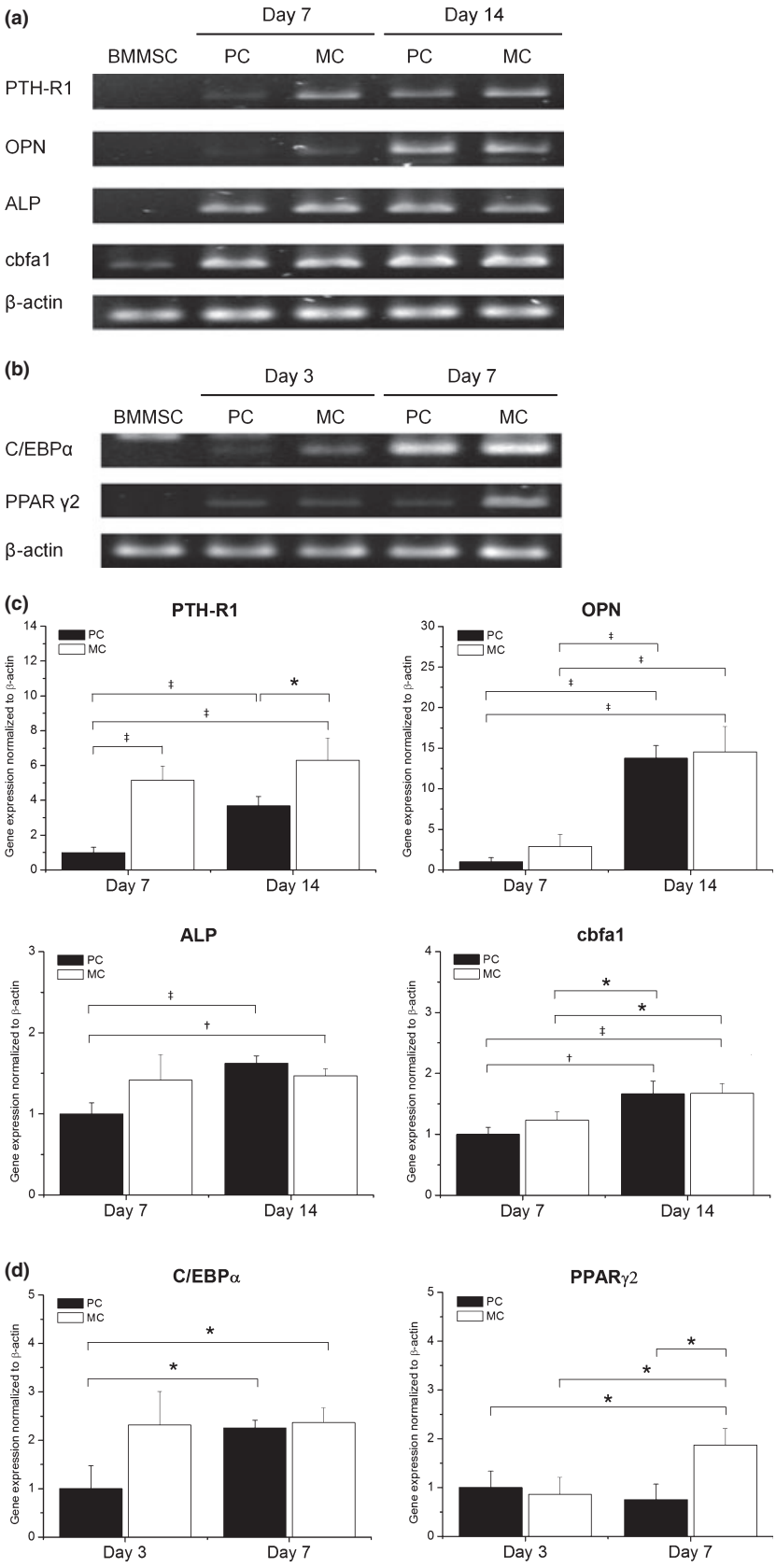

Figure 6. Effect of MC on osteogenic and adipogenic gene expression in BMMSCs. Electrophoresis of reverse transcriptase-polymerase chain reaction (RT-PCR) products of (a) osteo-differentiated and (b) adipo-differentiated BMMSCs. BMMSC lane indicates undifferentiated BMMSCs from PC (day 3). To examine changes in expression of (c) osteogenic and (d) adipogenic genes with time respectively, cells were harvested on indicated days and subjected to semi-quantitative RT-PCR followed by agarose gel electrophoresis and ethidium bromide staining. β-actin was amplified as internal control. RT-PCR amplification products quantified and values represent fold change relative to day 7 of PC (osteogenesis) or day 3 of PC (adipogenesis). Data points represent mean value ± SD ($n = 3$). *$P < 0.05$. †$P < 0.01$. ‡$P < 0.005$.

suggesting that BMMSCs cultured in stirred MC have a higher rate of oxidative phosphorylation than do cells grown in plate culture. Additionally, lower initial cell density resulted in higher $Y_{Lac/Glc}$. In agreement with this, higher $Y_{Lac/Glc}$ from MC bead-T was obtained after the second feeding, which may suggest that adaptation of BMMSCs to these conditions caused higher metabolic stress.

Increased expression of stromal cell-derived factor-1 by ischaemic myocardium attracts CXCR4 positive bone marrow-derived stem cells (27). In addition, higher CXCR4 expression in MSCs after transduction with retroviral vector containing CXCR4 increases cell migration toward stromal cell-derived factor-1 (28). Culturing MSCs for more than two passages results in reduced expression of adhesion molecules as well as loss of chemokine receptors including CXCR4 (29,30). In our analysis, BMMSCs cultured in PC and MC showed reduced levels of CXCR4 expression over time. This result confirms previous studies that showed down-regulation of CXCR4 expression during *in vitro* culture processes (29,30). Although reduced, BMMSCs from MCs had higher expression levels of CXCR4 than those from PCs at day 6. This result suggests that the MC process promotes culture of BMMSCs and also helps to maintain CXCR4 expression, which is involved in homing ability of stem cells.

Recently, up-scalability of MSCs in MC has been expanded with (serial) bead-to-bead transfer (15,31). Based on use of bead-to-bead transfer, the available surface area for cell population growth can be extended and culturing of anchorage-dependent cells can be prolonged as free cells from old beads colonize fresh beads (32). In our study, use of bead-to-bead transfer did, however, result in MSC confluence on old beads (data not shown) and the percentage of granular cells (C2 plus C4 division) was higher than that observed in PC or MC. However, activity of ALP-positive cells (BMMSC-derived osteoblasts) and percentage of cells containing lipid droplets (BMMSC-derived adipocytes) in differentiated BMMSCs from MCs bead-T were lower than for those from PCs and were also significantly lower than for those from MCs. In comparison with PC or MC bead-T, MC using a semi-continuous process enhanced both osteogenic and adipogenic differentiation of BMMSC.

MSCs are heterogeneous in morphology (22,33,34), and differentiation potential of MSCs may vary depending on their source (35) or variable culture conditions including differences in initial cell density (19,36). In BMMSC cultures, large cells are considered to be mature MSCs and smaller cells as recycling stem cells (22). Recycling stem cells replicate and give rise to mature MSCs, which become the predominant cell type as cultures approach senescence (23). In our study, BMMSCs recovered from PCs at day 3 displayed a variety of cell morphologies, whereas BMMSCs recovered from MCs at day 3 were much more homogeneous in size (Fig. 3a). By analysing cell size and granularity, we infer that MC increased percentage of small and agranular cells in the total BMMSC culture (Fig. 3b, C3 division), but MC also selectively reduced the subpopulation of very small and agranular cells among total BMMSC culture (Fig. 3b, B division). These different subpopulations of cells may account for differences between osteogenic and adipogenic differentiation potential among cells from PC and MC at day 3 and from MC bead-T at day 9.

In conclusion, stirred MC systems of CultiSpher-G provide higher specific surface area, ease of monitoring, and ability to scale-up human BMMSC culture without loss of differentiation potential. To achieve more homogeneous morphology and better differentiation potential for BMMSCs, semi-continuous MC of BMMSCs may be more beneficial than PC or MC bead-T methods.

References

1 Lysy PA, Campard D, Smets F, Malaise J, Mourad M, Najimi M *et al.* (2008) Persistence of a chimerical phenotype after hepatocyte differentiation of human bone marrow mesenchymal stem cells. *Cell Prolif.* **41**, 36–58.

2 Pittenger MF, Mackay AM, Beck SC, Jaiswal RK, Douglas R, Mosca JD *et al.* (1999) Multilineage potential of adult human mesenchymal stem cells. *Science* **284**, 143–147.

3 Abdallah BM, Kassem M (2008) Human mesenchymal stem cells: from basic biology to clinical applications. *Gene Ther.* **15**, 109–116.

4 Chang YJ, Liu JW, Lin PC, Sun LY, Peng CW, Luo GH *et al.* (2009) Mesenchymal stem cells facilitate recovery from chemically induced liver damage and decrease liver fibrosis. *Life Sci.* **85**, 517–525.

5 Otto WR, Rao J (2004) Tomorrow's skeleton staff: mesenchymal stem cells and the repair of bone and cartilage. *Cell Prolif.* **37**, 97–110.

6 Badet L, Benhamou PY, Wojtusciszyn A, Baertschiger R, Milliat-Guittard L, Kessler L *et al.* (2007) Expectations and strategies regarding islet transplantation: metabolic data from the GRAGIL 2 trial. *Transplantation* **84**, 89–96.

7 Janssens S, Dubois C, Bogaert J, Theunissen K, Deroose C, Desmet W *et al.* (2006) Autologous bone marrow-derived stem-cell transfer in patients with ST-segment elevation myocardial infarction: double-blind, randomized controlled trial. *Lancet* **367**, 113–121.

8 Banfi A, Bianchi G, Notaro R, Luzzatto L, Cancedda R, Quarto R (2002) Replicative aging and gene expression in long-term cultures of human bone marrow stromal cells. *Tissue Eng.* **8**, 901–910.

9 Derubeis AR, Cancedda R (2004) Bone marrow stromal cells (BMSCs) in bone engineering: limitations and recent advances. *Ann. Biomed. Eng.* **32**, 160–165.

10 Javazon EH, Beggs KJ, Flake AW (2004) Mesenchymal stem cells: paradoxes of passaging. *Exp. Hematol.* **32**, 414–425.

11 Frauenschuh S, Reichmann E, Ibold Y, Goetz PM, Sittinger M, Ringe J (2007) A microcarrier-based cultivation system for expansion of primary mesenchymal stem cells. *Biotechnol. Prog.* **23**, 187–193.

12 Rubin JP, Bennett JM, Doctor JS, Tebbets BM, Marra KG (2007) Collagenous microbeads as a scaffold for tissue engineering with adipose-derived stem cells. *Plast. Reconstr. Surg.* **120**, 414–424.

13 Yang Y, Rossi FM, Putnins EE (2007) Ex vivo expansion of rat bone marrow mesenchymal stromal cells on microcarrier beads in spin culture. *Biomaterials* **28**, 3110–3120.
14 Malda J, Frondoza CG (2006) Microcarriers in the engineering of cartilage and bone. *Trends Biotechnol.* **24**, 299–304.
15 Sart S, Schneider YJ, Agathos SN (2009) Ear mesenchymal stem cells: an efficient adult multipotent cell population fit for rapid and scalable expansion. *J. Biotechnol.* **139**, 291–299.
16 Sun LY, Hsieh DK, Yu TC, Chiu HT, Lu SF, Luo GH *et al.* (2009b) Effect of pulsed electromagnetic field on the proliferation and differentiation potential of human bone marrow mesenchymal stem cells. *Bioelectromagnetics* **30**, 251–260.
17 Lin PC, Chen YL, Chiu SC, Yu YL, Chen SP, Chien MH *et al.* (2008) Orphan nuclear receptor, Nurr-77 was a possible target gene of butylidenephthalide chemotherapy on glioblastoma multiform brain tumor. *J. Neurochem.* **106**, 1017–1026.
18 Sun LY, Hsieh DK, Lin PC, Chiu HT, Chiou TW (2009a) Pulsed electromagnetic fields accelerate proliferation and osteogenic gene expression in human bone marrow mesenchymal stem cells during osteogenic differentiation. *Bioelectromagnetics* **31**, 209–219.
19 Tropel P, Noel D, Platet N, Legrand P, Benabid AL, Berger F (2004) Isolation and characterization of mesenchymal stem cells from adult mouse bone marrow. *Exp. Cell Res.* **295**, 395–406.
20 Robison R (1923) The possible significance of hexosephosphoric esters in ossification. *Biochem. J.* **17**, 286–293.
21 Bobis S, Jarocha D, Majka M (2006) Mesenchymal stem cells: characteristics and clinical applications. *Folia Histochem. Cytobiol.* **44**, 215–230.
22 Colter DC, Class R, DiGirolamo CM, Prockop DJ (2000) Rapid expansion of recycling stem cells in cultures of plastic-adherent cells from human bone marrow. *Proc. Natl. Acad. Sci. USA* **97**, 3213–3218.
23 Digirolamo CM, Stokes D, Colter D, Phinney DG, Class R, Prockop DJ (1999) Propagation and senescence of human marrow stromal cells in culture: a simple colony-forming assay identifies samples with the greatest potential to propagate and differentiate. *Br. J. Haematol.* **107**, 275–281.
24 Ozturk SS, Palsson BO (1991) Growth, metabolic, and antibody production kinetics of hybridoma cell culture: 2. Effects of serum concentration, dissolved oxygen concentration, and medium pH in a batch reactor. *Biotechnol. Prog.* **7**, 481–494.
25 Hassell T, Gleave S, Butler M (1991) Growth inhibition in animal cell culture. The effect of lactate and ammonia. *Appl. Biochem. Biotechnol.* **30**, 29–41.
26 Lao MS, Toth D (1997) Effects of ammonium and lactate on growth and metabolism of a recombinant Chinese hamster ovary cell culture. *Biotechnol. Prog.* **13**, 688–691.
27 Brunner S, Winogradow J, Huber BC, Zaruba MM, Fischer R, David R *et al.* (2009) Erythropoietin administration after myocardial infarction in mice attenuates ischemic cardiomyopathy associated with enhanced homing of bone marrow-derived progenitor cells via the CXCR-4/SDF-1 axis. *FASEB J.* **23**, 351–361.
28 Bhakta S, Hong P, Koc O (2006) The surface adhesion molecule CXCR4 stimulates mesenchymal stem cell migration to stromal cell-derived factor-1 in vitro but does not decrease apoptosis under serum deprivation. *Cardiovasc. Revasc. Med.* **7**, 19–24.
29 Honczarenko M, Le Y, Swierkowski M, Ghiran I, Glodek AM, Silberstein LE (2006) Human bone marrow stromal cells express a distinct set of biologically functional chemokine receptors. *Stem Cells* **24**, 1030–1041.
30 Son BR, Marquez-Curtis LA, Kucia M, Wysoczynski M, Turner AR, Ratajczak J *et al.* (2006) Migration of bone marrow and cord blood mesenchymal stem cells in vitro is regulated by stromal-derived factor-1-CXCR4 and hepatocyte growth factor-c-met axes and involves matrix metalloproteinases. *Stem Cells* **24**, 1254–1264.
31 Schop D, Janssen FW, Borgart E, de Bruijn JD, van Dijkhuizen-Radersma R (2008) Expansion of mesenchymal stem cells using a microcarrier-based cultivation system: growth and metabolism. *J. Tissue Eng. Regen. Med.* **2**, 126–135.
32 Ohlson S, Branscomb J, Nilsson K (1994) Bead-to-bead transfer of Chinese hamster ovary cells using macroporous microcarriers. *Cytotechnology* **14**, 67–80.
33 Mets T, Verdonk G (1981) In vitro aging of human bone marrow derived stromal cells. *Mech. Ageing Dev.* **16**, 81–89.
34 Zohar R, Sodek J, McCulloch CA (1997) Characterization of stromal progenitor cells enriched by flow cytometry. *Blood* **90**, 3471–3481.
35 Tsai MS, Hwang SM, Chen KD, Lee YS, Hsu LW, Chang YJ *et al.* (2007) Functional network analysis of the transcriptomes of mesenchymal stem cells derived from amniotic fluid, amniotic membrane, cord blood, and bone marrow. *Stem Cells* **25**, 2511–2523.
36 Reyes M, Lund T, Lenvik T, Aguiar D, Koodie L, Verfaillie CM (2001) Purification and ex vivo expansion of postnatal human marrow mesodermal progenitor cells. *Blood* **98**, 2615–2625.